submitted manuscript. Layout mimicks the paper to be published. N.S. 2004 01 28

Full Paper: In part 1 of this series results of an in-situ small-angle X-ray scattering (SAXS) study of polyethylene crystallization are presented. They show that crystallite placement is basically a random process, from which some order is growing. This paper presents a first survey concerning the required change of paradigm.

No distortion of a lattice is to be studied, but order grown on the nanometer scale must be distinguished from the stochastic case, i.e. the "car parking problem" from the field of random sequential adsorption (RSA). RSA is explored by computer simulation. The results concerning the corresponding liquid scattering are required to identify short-range order (cf. part 3). Processing of simulated scattering patterns verifies that the features of quasi-random arrangement are preserved in the interface distribution function (IDF), if only the crystals are shielded by some transition layer.

In a condensed random nanostructure almost only next neighbor correlations are present. The distribution of the widths of amorphous gaps between the crystals, h_a, is a truncated exponential distribution. In the scattering pattern the stochastic nanostructure can hardly be distinguished from a system with short-range order. On the other hand, in the IDF the features of order become clear. In random systems there is no convolution polynomial based on crystalline and amorphous distributions. Only two shifted images of h_a are occurring. We find that packing correlations collapse, if the crystallite thickness distribution is wide enough. In this case the pure particle scattering is a fair approximation in the IDF. This criterion is, in general, valid for technical polymer materials.

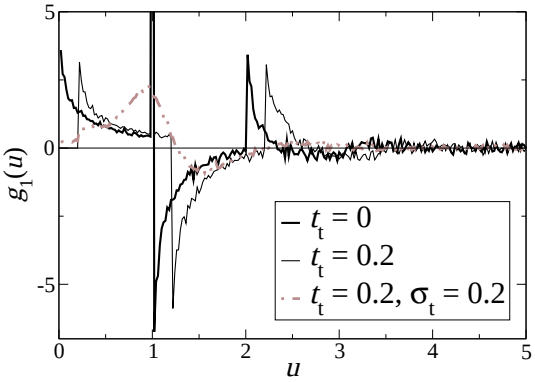

IDFs $g_1\,(u)$ computed from the nanostructure obtained in a computer simulation of ideal random isothermal crystallization after infinite time (random car parking process). **Bold line:** No transition zone. **Thin line:** Transition zone introduced ($\bar{p}_t/\bar{p}_c = \bar{t}_t/\bar{t}_c = 0.2$). **Dashed-dotted:** A Gaussian crystalline layer thickness distribution with a standard deviation of $\sigma_t = 0.2$.

Oriented quiescent crystallization of polyethylene studied by USAXS. Part 2: The liquid scattering of stacks generated by random placement of lamellae

Norbert Stribeck

Institute of Technical and Macromolecular Chemistry, University of Hamburg, Bundesstr. 45, 20146 Hamburg, Germany, Fax: +49 40-4123-6008, eMail: Norbert.Stribeck@desy.de

Keywords: crystallization; disorder; lamellar; SAXS; theory;

Introduction

The results of an in-situ SAXS study presented in part 1[1] of this series of papers on the crystallization of polyethylene show, that crystallization resembles the frequently studied process of random car parking.[2] Crystallite insertion on the shish (parking lane) is more or less random. Thus one should abandon the notion of a distortion of order (distorted lattice). Instead, the question is arising how a certain amount of order is accruing in face of a predominantly stochastic process. In other words, the formation of "lamellar stacks"[3] or "paracrystals"[4, 5] appears to be a second order process that only locally is breaking the random character of crystallite placement. Before we start to see into this phenomenon by analysis of scattering data (part 3), we first try to describe the ideal random process and its effects on nanostructure, small-angle X-ray scattering (SAXS) and the evaluation of scattering data.

Since Zernike and Prins[6] the scattering from particle systems with distorted order is studied. If the distortion grows exceedingly, order is vanishing. The particles are placed at random. If such or similar systems are studied, it is incorrect to describe them using notions valid for the description of lattice structures. Already Debye and Menke[7] moan that because of poor knowledge on liquids on one hand, but the perspicuous

theory of crystallography on the other, scientists become attracted to draw conclusions concerning structure based on the positions of interference maxima only.

Random placement does not necessarily mean that all phase relations among the particles are extinguished and we observe pure particle scattering. In practice, frequently broad maxima are observed and addressed by the term "liquid scattering". There is no such halo for some stochastic systems constructed by Porod,[8] but in distorted lattices considered by Hosemann[9, 10] liquid scattering is found. Now the question arises, if the observation of liquid scattering is necessarily going along with some rest of order, or if even a pure random process may generate liquid scattering behavior, if only the artificial construction of the early Porod model is abandoned. This question is of vital importance for the quantitative analysis of time-resolved SAXS studies of poorly ordered nanostructures. Only if the effect of those correlations that are enforced by dense packing can be considered and subtracted if necessary, an order generating process in the course of nanostructure formation can be detected and identified.

Since the early days of statistical physics the problems of liquid scattering has intensively been studied. To date both several approximations and some closed form solutions are known. Most frequently applied[11–16] is the Percus-Yevick[17] approximation of the Ornstein-Zernike integral equation. It offers a simple description of the scattering generated from systems with short-range order. Nevertheless, its basic modeling is a coarse approximation[18] only, based on a notion of liquid scattering that does not really cover the process observed in the experiment.

For isothermal crystallization the definition of the ideal random process is obvious, if crystalline domains (kebab) are growing on a backbone (shish): Crystal lamellae are generated at random positions on the shish. The process is continued, until the last gap of sufficient size is filled by a crystal ("jamming limit"). For lamellae of uniform thickness this process is known as the "car parking problem", one of the many problems discussed in the field of random sequential adsorption (RSA).[2] For the ideal case the correlation function describing the statistical arrangement of uniform lamellae has been derived in closed form by Bonnier, Boyer and Viot.[18]

Theoretical

General considerations

Uniform crystals in one dimension. Let us consider an isothermal crystallization process of polymers starting from random places on a backbone (shish), during which only crystallites of uniform thickness are generated. Let the crystallite thickness, $\bar{t}_c = \bar{p}_c\, r_m$, be exactly $\bar{p}_c$ monomer units (ideal isothermal crystallization) with r_m the length of one monomer. Thus the crystal thickness distribution, $h_c\,(p) = \delta\,(p - \bar{p}_c)$ is a δ–distribution.

Random packing and truncated amorphous thickness distribution. In the beginning of random crystallization along a shish, the distances between crystals are uniformly distributed, but in the course of time the number of places is decreasing, at which another crystal can develop. Finally, all the gaps that would have room for a crystal are occupied, and the distribution of amorphous thicknesses, $h_a\,(r_3)$, has developed from a constant to a random variable defined over a finite interval, a truncated probability distribution.[19, 20]

Questions to be answered. Here several questions arise. How does this distribution look like? Does it imprint correlations among the domains? Which is the natural volume crystallinity, v_{cs}^{∞}, of ideal random isothermal crystallization? In the literature of applied mathematics that is dealing with the development of truncated distributions in the case of iterated stochastic processes in several fields of science,[19–22] several heuristic descriptions can be found. It is frequently reported that the emerging distributions are from the class of exponential functions.

Answers from statistical mathematics and physics. In statistical mathematics and physics the ideal random process described above is known as the "car parking problem".[2] Its kinetics and some of its properties has first been studied by Rényi[23](translated[24]). For example, the natural volume crystallinity

$$v_{cs}^{\infty} = 2\int_0^{\infty} \exp\left[-t - 2\int_0^{t} \frac{1-\exp\left(-u\right)}{u}\, du\right]\, dt = 0.747\,597\,92 \tag{1}$$

of the "jammed state" is known as the Rényi limit. It says that if 75% of the length of a parking lane are filled by cars parked randomly, there will be no more space to put another. A review concerning theory and applications in the corresponding fields of random sequential adsorption (RSA) and cooperative sequential adsorption (CSA) has been published by Evans.[2] For the car parking statistics Bonnier, Boyer and Viot[18] have deduced both the correlation function and the static structure factor in closed form. Nevertheless, the equations given by them are infinite series of nested integrals that, to the best of our knowledge, require considerable computational effort. Moreover, the practically relevant case of a broad crystallite thickness distribution is not covered.

Description of the stochastic process

If, for the random crystallization, we intend to acquire a heuristic description of $h_a\,(r_3)$, we need an experiment under ideal conditions. Such ideal conditions can be provided in a computer simulation[25] of one-dimensional, ideal, and isothermal crystallization. Here we assume that the crystallite thicknesses are quantized by the monomer lengths of the polymer chains.

Then, in a series of computer simulations, we determine the arrangement of the crystals on a shish after a very long crystallization time. The crystallite thickness, $\bar{t}_c = r_m\,\bar{p}_c$ is varied in integer steps of the number of monomers, $\bar{p}_c = [1, 2, 3, \ldots]$, straddling the lamella.

Computer simulation technique. Random numbers are generated by means of the pseudo random number generator of Borland Pascal 7.0, the quality of which is improved by random shuffling.[26,27] Using the generator in a loop, random numbers are generated, which represent crystallite positions on a shish. If there is room for the crystal at that position, a crystal record is generated and inserted into a circular list. At any time this list represents the shish and the crystals existing. As long as all the crystal sizes are identical, this process is stable and stops when the jamming limit is reached. Because of the computing speed available to date, the transformations described in the paper of Burgos and Bonadeo[25] are no longer required.

Gaussian crystallite thickness distributions are generated by channeling our uniform random numbers through the Box-Muller transform.[28,29] Here a fundamental problem becomes obvious: as soon as the shish is sufficiently structured, thin crystallites are more easily inserted than thick ones, and in the course of time the crystal fraction is drifting towards 1. In addition, Gaussians are problematic to use because of their wide tails. We have prohibited the creation of crystallites with negative thickness and have stopped the corresponding simulation after a crystallinity of 65% was reached.

The computer program is compiled under Linux in order to take advantage of its superior memory management. The list of crystals and the huge array for the IDF require an extended heap of 40 MB size. With about 20000 crystals generated on a shish offering room for 32000 crystals, a typical run is finished after 10 min.

The amorphous thickness distribution. For the distribution of the amorphous thicknesses, h_a, we find by fitting to the results of the computer simulations

$$h_a(u) = \frac{1}{N}\,\exp\left(-\frac{2}{3}\pi\sqrt{u}\right), \quad u \in (0,1), \tag{2}$$

with $u = r_3/\bar{t}_c$. Postulating $\int h_a(u)\,du = 1$ as we have implicitly done for the crystallite thickness distribution, then it follows

$$N = \frac{9\,(\exp(2\,\pi/3) - 1) - 6\,\pi}{2\,\pi^2\,\exp(2\,\pi/3)}, \tag{3}$$

and the center of gravity of $h_a(u)$ is

$$\langle h_a(u)\rangle = \frac{4\,\pi^3 + 18\,\pi^2 + 54\,\pi + 81\,(1 - \exp(2\,\pi/3))}{2\,\pi^2\,(2\,\pi + 3\,(1 - \exp(2\,\pi/3)))}. \tag{4}$$

The ultimate statistical crystallinity. The ultimate crystallinity v_{cs}^{∞} (i.e. the maximum crystallinity achieved for the case of ideal random crystallization from crystals of uniform thickness after infinite time) is

$$v_{cs}^{\infty} = \frac{1}{1 + \langle h_a(u)\rangle} = 0.74, \tag{5}$$

a value very close to the theoretical Rényi limit (Equation 1 and[2,24]). Because of the quantization of the crystallite thicknesses this ultimate value is only reached for very thick lamellae (cf. Figure 1).

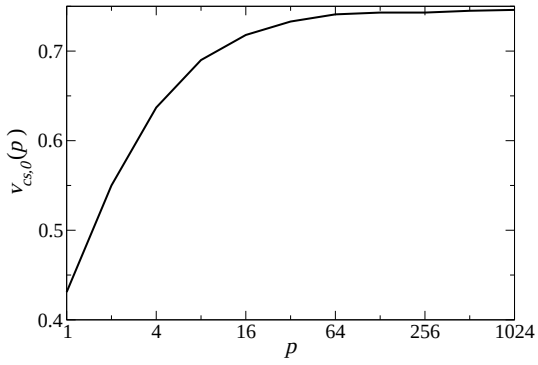

Figure 1: The limiting volume crystallinity of statistical isothermal crystallization, $v_{cs,0}\,(p)$, as a function of the crystallite thickness, p, measured in monomer units (logarithmic scale). Data resulting from computer simulations.

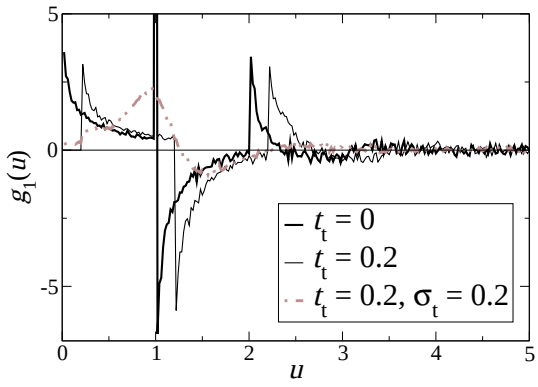

Figure 2: IDF $g_1\,(u)$ computed from the nanostructure obtained in a computer simulation (ideal isothermal crystallization for infinite time). Curves are normalized to represent the scattering effect of 1 lamella of electron density contrast 1 ($\Delta\rho = \rho_c - \rho_a = 1$). **Bold line:** No transition zone. $N_c = 11817$ crystals of thickness $\bar{p}_c = 50$: monomer units grown on a shish of length 16000*50 until there was no more room for new crystals. Volume crystallinity $v_{cs} = 11817/16000 = 0.74$. **Thin line:** Transition zone introduced ($\bar{p}_t/\bar{p}_c = \bar{t}_t/\bar{t}_c = 0.2$). **Dashed-dotted:** A Gaussian crystalline layer thickness distribution with a standard deviation of $\sigma_t = 0.2$.

Correlations after random packing of uniform crystals. Now that we know the distance distribution h_a of amorphous layers, we could further on adhere to Hermans's[3] model developed by distorting a perfect periodical structure, assume that all distances are statistically independent of each other, and generate the infinite series of distance distributions, a convolution polynomial. The superposition of all the contributions generated in this manner would be an IDF, $g_1\,(r_3)$.

Nevertheless, for a stochastic system we are extremely far from an ordered system. So we should be cautious and compute $g_1\,(r_3)$ from the exact solution[18] or from the nanostructure generated in our simulations directly using the positions of the crystals on the shish. For this purpose we mark each left edge of a crystal on the shish by a 1, each right edge by a -1. Finally, from the series of δ-distributions developed in this way we compute the autocorrelation. Three of the results are demonstrated in Figure 2.

In the figure (cf. as well Hosemann,[10] Figure 3) the IDF is plotted as a function of the relative crystallite thickness, u, and normalized to the scattering effect of a single lamella. The bold line shows the result for a case, in which no transition zone ($t_t = 0$) to the left and to the right of the lamella is assumed. Thus crystallites can be put arbitrarily close to each other. The thin line demonstrates a case, in which 20% of the crystallite thickness are declared inaccessible around the crystal ($t_t/\bar{t}_c = 0.2$). This becomes physically meaningful, if we furnish a transition layer[30,31] in this gap, in which the density slowly drops to the density of the amorphous phase.

In the dilute system, only the δ-function of the crystallite thickness distribution would be observed at $u = 1$. The simulation demonstrates, however, that in the concentrated system additional terms arise in $g_1\,(u)$, which cause liquid scattering. These terms shall be denoted "packing correlation". The packing correlation has several characteristics:

1. Packing correlation is shifted by $t_t/\bar{t}_c$, if a transition layer is considered.

2. Packing correlation is of extremely short range. For distances $u > 3 + t_t$ it vanishes even along the crowded backbone.

3. If the crystal thicknesses are no longer uniform (dashed-dotted curve), the packing correlation is strongly attenuated. The positive correlation peak to the right of the long period peak vanishes already, if the width of the crystallite thickness distribution is relatively narrow.

4. In the scattering pattern packing correlation causes a strong maximum ("long period peak") and a series of undulations, which at least become visible in a plot that linearizes Porod's law (this property is demonstrated below in Figure 4).

The terms of packing correlation. Essentially left of the δ–peak describing the h_c–distribution we recognize in each case the truncated exponential distribution of the amorphous gaps, $h_a\,(u - t_t/\bar{t}_c)$. The negative peak to the right of the h_c–peak is caused from the long periods $h_L\,(u) = h_{ac}\,(u)$, (i.e. the distance from the end of a crystal to the end of its neighbor). Because the crystallite thickness distribution is ideal, here the distribution of the amorphous thicknesses is replicated ($h_L\,(u) = -2\,h_a\,(u - t_t/\bar{t}_c - 1)$). The factor 2 arises, because the distances from the beginning of a crystal to the beginning of its neighbor are subjected to the same statistics. Even further to the right we, again, find an image of the h_a–distribution. It is caused from the sandwiches made from two crystallites and an amorphous layer in between, $h_{cac}\,(u) = h_a\,(u - t_t/\bar{t}_c - 2)$.

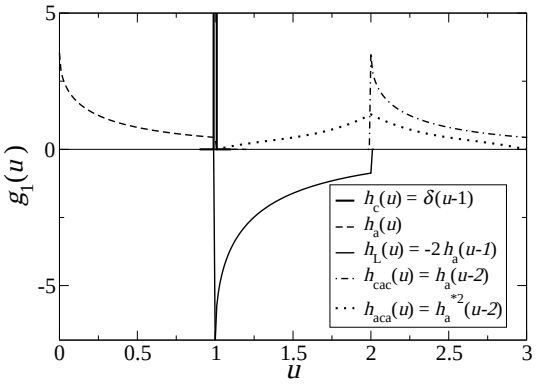

Figure 3: Random packing of uniform crystallites without interfacial layer. Sketch of the low-order distance distributions, $h_i\,(u)$ which form an IDF $g_1\,(u)$. $u = r_3/\bar{t}_c$, and $\bar{t}_c$: crystal thickness

No convolution polynomial. For clarity, Figure 3 shows the components separately for the simple case of a shish that is randomly and fully ($t_t = 0$) laden with uniform crystals. In addition, the sketch shows a distribution h_{aca} (dotted line). For this example h_{aca} is the first distribution that, according to the notion of distorted order,[3] is computed by convolution ($h_{aca} = h_a * h_a$). Comparison with the IDFs from the ideal random crystallization (Figure 2) readily exhibits that a a triplet distribution h_{aca} is much weaker as it would have to be if it were constructed by convolution.

Thus, on the crowded stochastic shish the crystalline lamellae sense nothing but their direct neighbors. Beyond that only a very weak and unspecifically fading signal is observed. As a result, the stochastic system is rather clearly distinguished from its packing correlation in the IDF. In the scattering pattern distinction is more difficult, but there is an example published in the literature where extremely low correlation among lamellae with clusters of less than two members has been deduced from direct analysis of scattering curves.[32]

A possibility to determine the width of the transition zone? It is worth to be noted that the width of the transition zone at the edges of the lamellae has a strong effect on the ultimate packing crystallinity (i.e. Rényi's limit). For $t_t = 0$ one readily obtains $v_{cs,0} = N_c/N_s$, with the number of generated crystals, N_c, and the length of the shish, $N_s = L_s/\bar{t}_c$, measured in units of the thickness of the crystalline lamellae. For the ultimate crystallinity with uniform crystals having a transition zone ($t_t > 0$) it follows

$$v_{cs} = \frac{v_{cs,0}}{1 + t_t/\bar{t}_c}. \tag{6}$$

Thus, as long as only crystals of uniform thickness are generated during random crystallization, the transition layer thickness t_t is coupled to the measured crystallinity and the crystallite thickness as measured in monomer units (Figure 1).

However, as soon as a Gaussian crystallite thickness distribution is considered, the amorphous gaps can be filled so well with small crystals in the computer simulation that both the shape of the crystal thickness distribution found on the shish is changing and Equation 6 is no longer valid.

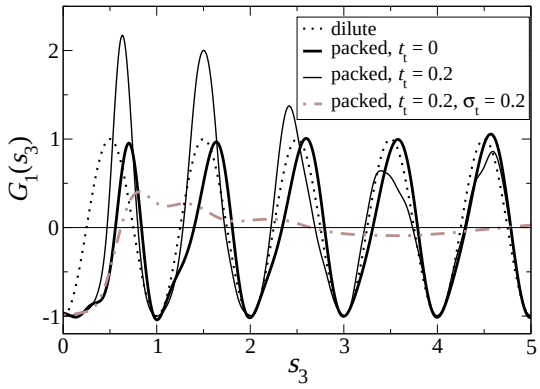

Figure 4: Interference functions, $G_1(s_3)$, for the random placement of layers of thickness 1 on a shish (normalized to the scattering effect of 1 layer with $\Delta\rho = 1$). **Dotted curve:** For sparse population on the shish. **Bold solid line:** For the densely packed system after infinite isothermal crystallization. **Thin solid line:** For the packed system, now assuming that each layer is enclosed in a transition layer of 20% the crystallite thickness. **Dot-dash-dotted:** Lamellae from a broad layer thickness distribution randomly packed.

From the simulated nanostructure to the scattering pattern

The interference function. After having studied the influence of packing correlation to the interface distribution function it appears meaningful to compare the related scattering curves to the scattering of the dilute system. Let $u = r_3$, and let us consider the case, in which the IDF $g_1(r_3)$ in meridional direction of a multidimensional scattering pattern is studied. Then the negative Fourier transform of the IDF is the one-dimensional interference function $G_1(s_3)$,[33] which differs from the static structure factor discussed by Bonnier, Boyer and Viot[18] by only a constant. Subjecting the examples of Figure 2 to the transformation, we yield the results shown in Figure 4.

Not long period maxima, but form factor minima characterize a packed random system. The dilute system of lamellae placed randomly (dotted curves) shows the expected harmonic curve $G_1(s_3) = -\cos(2\pi\bar{t}_c s_3)$ with $\bar{t}_c = 1$. After crowding the shish with lamellae (bold solid line), packing correlation leads to a different interference function. Again considerable changes are found, if the crystal lamellae are wrapped in a transition zone (thin solid line).

For uniform lamellae at high orders all the interference functions become identical and show that the placement is, indeed, random. Nevertheless, in experimental SAXS data this information is inaccessible, because noise and the practical variation of crystal thickness suppress this information (dot-dash-dotted line).

On the other hand, in the accessible region peak shapes and positions are changing as a function of packing density. If we adopt the paradigm of distorted order and analyze SAXS curves of systems with predominantly random nanostructure, we will presumably discuss shapes and positions of peaks. Then we will hardly retrieve meaningful results. On the other hand, the model calculations demonstrate that the particle factor minima are preserved – as long as no crystallite size distribution must be considered (dot-dash-dotted line). The interference function obtained in the simulation for non-uniform crystal thicknesses is similar to data frequently reported in experimental SAXS studies. From the inclination of the linear region (Porod's law, $1 < s_3 < 3$) the transition layer thickness t_t is retrieved.

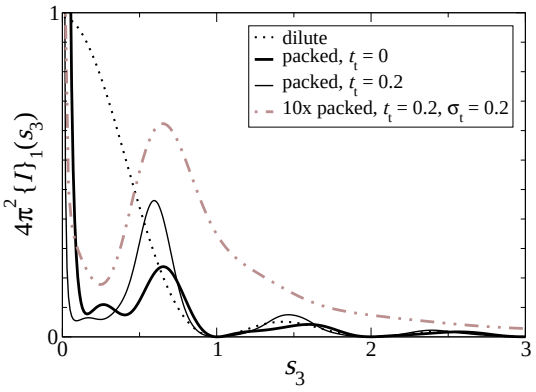

Figure 5: Liquid scattering projected on the meridian, $\{I\}_1(s_3)$, for random placement of $4\pi^2$ crystallites with with $\Delta\rho = 1$ on a shish. Note the positions of the minima and the varying strength of the oscillations.

The scattering patterns. Now, from the interference functions, the scattering curves projected on the meridian,

$$\{I\}_1(s_3) = \left(4\pi^2 s_3^2\right)^{-1} (G_1(s_3) + 1)$$

are computed. These functions are the Lorentz-corrected scattering curves of an isotropic lamellar system. Thus the connection of these considerations to an experiment is made, in which the nanostructure of an uniaxially highly oriented semicrystalline sample is studied by means of SAXS and a two-dimensional detector. A selection of the scattering curves expected for random placement of lamellae is shown in Figure 5.

The observation of peaks in the presented scattering curves of the condensed systems is not related to order. As already stated by Hosemann,[10] an emerging long period in a stochastic system only indicates the transition from a diluted to a concentrated system. If, moreover, a broad crystallite size distribution is considered, we find a scattering curve with a peak but without particle factor minima. Similar curves are reported in many SAXS studies.

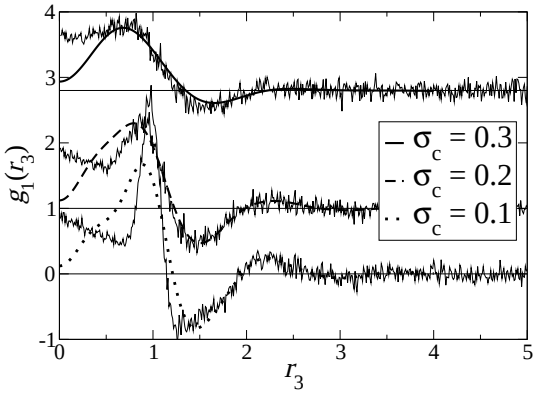

Figure 6: Comparison of original IDFs used to generate simulated scattering curves (noisy data) and the results of data analysis (smooth curves). Average crystalline thickness, $\bar{t}_c = 1$. No transition layer.

Data evaluation of simulated scattering curves

For the evaluation of scattering data we utilize our method of spatial frequency filtering[34,35] and retrieve the nanostructure information as a CDF or an IDF. If we work with scattering patterns of nanostructures with a certain amount of order, we know that our method is able to extract the requested topological information with high accuracy.

If now we start to evaluate stochastic nanostructures we need to check the efficiency of the procedure for such structures as well. For this purpose we have, first, applied typical experimental noise to the scattering curves computed from the simulated stochastic structures. Afterwards we have evaluated these curves in exactly the same way as the data from our crystallization experiments.[1,36] By comparison with the input data we then can estimate how careful nanostructure information is treated by the evaluation method. The results for crystals put on the shish without a transition layer are shown in Figure 6.

The reproducibility of the structure information (noisy data) after analysis (smooth curves) is not sufficient. The reason for this result is the fact that the distribution h_a of the amorphous gaps does not vanish at $r_3 = 0$. As a consequence, the spatial frequency filter assigns part of h_a to the diffuse background scattering and removes it. If, on the other hand, a transition zone $t_t > 0$ is present, the nanostructure information is well preserved (Figure 7).

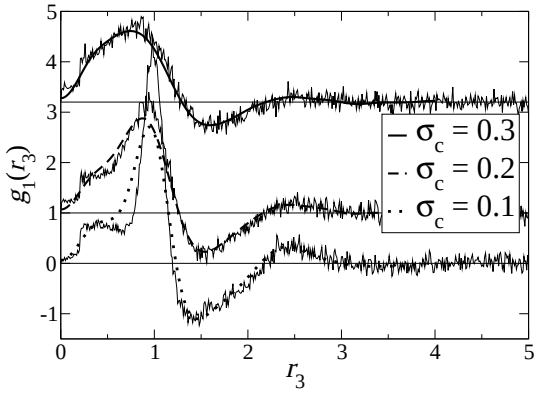

Figure 7: Comparison of original IDFs used to generate simulated scattering curves (noisy data) and the results of data analysis (smooth curves). Average crystalline thickness, $\bar{t}_c = 1$. Transition zone width $t_t = 0.2$

Because we can usually assume that a transition zone is present, the conditions shown in Figure 7 are close to the common situation. Here only the narrow crystallite thickness distribution ($\sigma_c = 0.1$) is broadened in the analysis. In the study of technical polymer products such narrow distributions will hardly appear. If, on the other hand, materials with extremely narrow molecular mass distributions or in extreme states are studied, one should be aware of the limits of established data evaluation technique.

Modeling the random crystallization with broad crystallite thickness distribution

Figure 7 as well shows that upon introduction of broad crystal thickness distributions the related packing correlations are virtually collapsing. A mathematical description for this phenomenon was not found. Nevertheless, some considerations shall be indicated. Already a small rise in relative standard deviation to 0.1 results in loss of the exponential character of the h_a–distribution. We only observe a diffusely truncated, almost uniform distribution $h_a(u) \approx 1, \quad u \in [t_t, t_t + 1]$. With such a model we can fit the initial part of our curves sufficiently well. The problem arises from the other two distri-

butions which contribute to packing correlation. Bearing in mind established notions, one may define these distributions by convolutions $h_{ac} = -2\, h_a * h_c$ and $h_{cac} = h_c * h_a * h_c$, respectively. Moreover, since crystal positioning is at random, an undisturbed superposition of random shishs with each a uniform crystallite thickness could be accepted (and modeled by Mellin convolution[37]). Neither these ideas nor their combination are able to describe the observed collapse of correlation found in the simulated random shish with wide crystallite thickness distribution. On the other hand, just this considerable collapse of correlations helps to establish a simple analysis procedure.

Negligibility of packing correlations. In Figure 7 for both the narrow crystallite thickness distributions packing correlations are clearly discernible, whereas they are only weak for the random nanostructure with $\sigma_c = 0.3$. Thus, for $\sigma_c \geq 0.3$ the correlations arising from liquid scattering are almost negligible as compared to the particle factor represented by the crystallite thickness distribution h_c. Hosemann[10] deduces a similar result for the three-dimensional case. According to his work liquid scattering is negligible for

$$g_y \geq \varepsilon^3.$$

Hosemann defines $g_y = \sigma_c/\bar{t}_c$, and his packing density ε is our crystallinity v_{cs} on the shish.

Form factor fitting. Technical polymer materials show, in general, no crystal thickness distributions with relative standard deviations below 0.3. So we have fitted the critical random shish scattering using the pure form factor and an infinite stack that was supplied in order to swallow remnant packing correlations. The result is shown in Table 1.

Table 1: Fits of packing correlation with the form factor of the ensemble of crystalline lamellae. Parameters are the standard deviation, σ_c, of the crystallite thickness distribution, the mean crystal thickness, $\bar{t}_c$, and the number fraction of lamellae in the uncorrelated shish. The column labeled "in" shows the input parameters for the simulation of the nanostructure, "out" shows the result of the simple form factor fit.

	in	out
σ_c	0.3	0.28
$\bar{t}_c$	1	1.00
W	1	0.72

	in	out
σ_c	0.4	0.39
$\bar{t}_c$	1	0.96
W	1	0.74

Obviously, the structural parameters are reproduced in the fit. On the other hand, because of the remnant liquid scattering a small fraction of the random crystals still is considered correlated.

Conclusions

We have learned that the crystallization of domains (kebab), randomly placed on a backbone (shish), always lead to packing correlation, if the system can not be considered diluted. Nanostructured polymer materials are, in general, concentrated systems. If for such materials the scattering intensity (projected on the meridian) is considered, it is difficult to discriminate, if the observed long period peaks result from distorted order (stack, lattice) or are nothing but liquid scattering. If the positions of peak maxima cannot easily be reduced to multiples of a first order, but the positions of minima can, this is indicative for packing correlation and liquid scattering. In this case the position of the first minimum is the inverse of the average crystallite thickness, and the crystallite thicknesses are nearly uniform.

In the IDF, on the other hand, ordered placement is clearly distinguished from mere packing correlation. If a narrow crystal thickness distribution peak is observed, packing correlation is dying out within the range of triple the room required for the placement of a crystal (in terms of RSA: "required for parking a car"). Every oscillation beyond this point indicates ordered placement. If the first maximum in the IDF is broad, already a positive peak to the right of the negative "long period peak" indicates a fraction of crystals that are placed by some ordering process.

The analysis of simulated scattering data from stochastic systems shows that caution is required if samples with narrow crystallite thickness distributions shall be analyzed. For technical materials with sufficiently broad crystallite thickness distributions and shielding by a transition zone the established data analysis methods appear to be sufficiently accurate.

Acknowledgments. I acknowledge the Deutsche Elektronen Synchrotron (DESY) for provision of synchrotron radiation facilities at HASYLAB within the frame of the project II-01-041. I would like to thank S. Cunis for assistance in using beamline BW4, and Dr. R. K. Bayer for the preparation of the polyethylene samples with unique orientation of the amorphous network, which were studied in the crystallization experiments that initiated this work.

References

[1] N. Stribeck, A. Almendarez Camarillo, S. Cunis, R. K. Bayer, R. Gehrke, *Macromol. Chem. Phys.* **2004**, *submitted*.
[2] J. W. Evans, *Rev. Mod. Phys.* **1993**, *65*, 1281.
[3] J. J. Hermans, *Rec. Trav. Chim. Pays-Bas* **1944**, *63*, 211.
[4] R. Hosemann, *Polymer* **1962**, *3*, 349.
[5] R. Hosemann, S. N. Bagchi, *Direct Analysis of Diffraction by Matter*, North-Holland, Amsterdam, **1962**.
[6] F. Zernike, J. A. Prins, *Z. Phys.* **1927**, *41*, 184.
[7] P. Debye, H. Menke, *Erg. techn. Röntgenkunde* **1931**, *2*, 1.

[8] G. Porod, *Kolloid-Z.* **1951**, *124*, 83.
[9] R. Hosemann, *Z. Phys.* **1949**, *127*, 16.
[10] R. Hosemann, *Kolloid Z.* **1950**, *117*, 13.
[11] D. J. Kinning, E. L. Thomas, *Macromolecules* **1984**, *17*, 1712.
[12] A. Santos, S. B. Yuste, M. López de Haro, *J. Chem. Phys.* **2002**, *117*, 5785.
[13] T. Kamiyama, M. Sasaki, K. Suzuki, *J. Appl. Cryst.* **2000**, *33*, 447.
[14] T. Kamiyama, K. Suzuki, *J. Non-cryst. solids* **1998**, *232-234*, 476.
[15] D. Boyer, G. Tarjus, P. Viot, *J. Chem. Phys.* **1995**, *103*, 1607.
[16] Y. Cohen, E. L. Thomas, *J. Polym. Sci., Part B: Polym. Phys.* **1987**, *B25*, 1607.
[17] J. K. Percus, G. J. Yevick, *Phys. Rev.* **1958**, *110*, 1.
[18] B. Bonnier, D. Boyer, P. Viot, *J. Phys. A* **1994**, *27*, 3671.
[19] P. Kumar, *J. Inequal. Pure and Appl. Math.* **2002**, *3*, art. 41.
[20] N. Balakrishnan, S. S. Gupta, in: C. R. Balakrishnan, N.; Rao, Ed. "Handbook of Statistics", Elsevier, Amsterdam, vol. 17, **1998** pp. 25–59.
[21] R. Aggarwala, N. Balakrishnan, *Ann. Inst. Statist. Math.* **1996**, *48*, 757.
[22] P. Varghese, R. Braswell, B. Wang, C. Zhang, *Comput. Aided Des.* **1996**, *28*, 723.
[23] A. Rényi, *Publ. Math. Inst. Budapest* **1958**, *3*, 109.
[24] A. Rényi, *Sel. Transl. Math. Stat. Prob.* **1963**, *4*, 203.
[25] E. Burgos, H. Bonadeo, *J. Phys. A* **1987**, *20*, 1193.
[26] D. W. Deley, "How Computers Generate Random Numbers", http://home1.gte.net/deleyd/random/introduction.htm, **1991**.
[27] L. Sim, K. Nitschke, *Austral. Phys. Eng. Sci. Med.* **1993**, *16*, 22.
[28] E. F. Carter, "Generating Gaussian Random Numbers", http://www.taygeta.com/random/gaussian.html.
[29] G. E. P. Box, M. E. Muller, *Annals Math. Stat.* **1958**, *29*, 610.
[30] W. Ruland, *J. Appl. Cryst.* **1971**, *4*, 70.
[31] C. G. Vonk, *J. Appl. Cryst.* **1973**, *6*, 81.
[32] H. G. Kilian, W. Wenig, *J. Macromol. Sci. - Phys.* **1974**, *B9*, 463.
[33] W. Ruland, *Colloid Polym. Sci.* **1977**, *255*, 417.
[34] N. Stribeck, *J. Appl. Cryst.* **2001**, *34*, 496.
[35] N. Stribeck, *Colloid Polym. Sci.* **2002**, *280*, 254.
[36] N. Stribeck, A. Almendarez Camarillo, R. Bayer, *Macromol. Chem. Phys.* **2004**, *submitted*.
[37] N. Stribeck, *Colloid Polym. Sci.* **1993**, *271*, 1007.

Synopsis. It is no use to interpret nanostructure data in terms of perfect order, if nature places crystalline lamellae preferentially at random positions. Instead, order generating processes are to be identified in a chaos, which unfortunately generates discrete scattering simply by packing the crystallites (car parking problem). The properties of the corresponding correlation among the crystallites are explored by computer simulation.

Polyethylene crystallizes in the form of plate-lets (lamellae) with a unit cell similar to that of low molecular mass parafn waxes [24]. Due to chain folding, the molecular axes are oriented perpendicular to the longest dimension of the lamella and not parallel to it as might be expected (Fig. 2). The thickness of the lamellae is deter-mined by the crystallization conditions and the concentration of branches and is typically in the range of 8 â€“ 20 nm. Thicker lamellae are asso-ciated with higher melting points and higher overall crystallinities.Â The typical milkiness of polyethylene is due to light scattered by spherulites or other, less well dened aggregates of crystallites, rather than by the crystallites themselves, which are much smaller than the wavelength of light [27]. Keywords: crystallization of polymers, in silico study, dissipative particle dynamics, semiexible polymers. arXiv:1708.09499v3 [physics.chem-ph] 28 Jan 2020. I. INTRODUCTION. Crystallization of polymer materials inuences strongly their macroscopic properties and plays an important role in many applications1â€“7. Understanding of polymer crystalliza-tion on the molecular level is one of the most challenging un-solved problem in modern polymer physics.Â One polymer bead in our model resembles a part of a polymer chain consisting of several monomer units, and one bead of a solvent includes several solvent molecules. Beads are interacting by pair-wise conservative force, dissipa-tive force and random force: â^‘. Please accept it and choose your preferences by ticking the corresponding boxes in the "Manage Settings" section below. Please carefully read our Terms of Service before you proceed with using any part of this website. Allow cookies. Manage Settings.Â 2.1 Clinical trials should be conducted in accordance with the ethical principles that have their origin in the Declaration of Helsinki, and that are consistent with GCP and the applicable regulatory requirement(s). 2.2 Before a trial is initiated, foreseeable risks and inconveniences should be weighed against the anticipated benefit for the individual trial subject and society. A trial should be initiated and continued only if the anticipated benefits justify the risks.